Validity of LiPON Conductivity Determined by Impedance Spectroscopy

Alexander Rudy *, Alena Novozhilova , Julia Egorova

Posted Date: 23 April 2024

doi: 10.20944/preprints202404.1506.v1

Keywords: solid electrolyte; impedance spectroscopy; absorption current; electric double layer; Debye length; drift conductivity

 doi:10.20944/preprints202404.1506.v1

Article

Validity of LiPON Conductivity Determined by Impedance Spectroscopy

Alexander Rudy [1,*], Alena Novozhilova [2] and Julia Egorova [1]

[1] P.G. Demidov Yaroslavl State University, rudy@uniyar.ac.ru
[2] Peoples' Friendship University of Russia named after Patrice Lumumba, alena.novozhilova.2014@mail.ru
* Correspondence: rudy@uniyar.ac.ru

Abstract: A hypothesis that the generally accepted value of the LiPON conductivity should be attributed to the absorption and displacement currents is substantiated. The reason is a small contribution of the drift current due to field screening by the electric double layer. The basis for this assumption is the measurement of the LiPON absorption capacitance, according to which its dielectric constant is about 10^6. An alternative equivalent circuit containing a non-ideal absorption element is proposed and its impedance is calculated. It is shown that the Bode diagrams of the alternative circuit well approximate the experimental curves. Parameters and the magnitude of electric field screening are calculated basing on proposed model of a double electric layer. Considering the screening effect, the drift conductivity of LiPON is obtained, which value is in good agreement with the data on lithium concentration and mobility.

Keywords: solid electrolyte; impedance spectroscopy; absorption current; electric double layer; Debye length; drift conductivity

1. Introduction

Solid-state thin-film lithium-ion batteries are a relatively new and promising type of chemical energy storage device. In the vast majority of these batteries as the solid electrolyte lithium phosphorus oxynitride (LiPON), developed in the mid-1990s by J. Bates et al. at Oak Ridge National Laboratory, is used. The most important LiPON characteristics were published by J. Bates et al. in [1–7]. In particular, in the very first work [1] the value of conductivity $\sigma=2\cdot10^{-6}\,\mathrm{S\cdot cm^{-1}}$ was reported. Later, these results were confirmed by subsequent works by J. Bates et al., as well as experimental [8–15] and theoretical [16] studies by other authors. In all cases, conductivity was understood as drift conductivity, which characterizes the ability of the electrolyte to transport lithium ions. It is shown below that, for a number of reasons, the obtained conductivity values must be attributed to the absorption current.

This follows from the results of [17] where the capacity of a Pt|LiPON|Pt sandwich structure with an area of $S=0.64\,\mathrm{cm^2}$ and a thickness of $d=1\,\mu\mathrm{m}$ was measured using the circuit displayed in Figure 1a. The voltage across the structure versus time is shown in Figure 1b. The LiPON chemical capacity was calculated as

$$Q=\frac{U_0}{R_0}T-\left(\frac{1}{R_0}+\frac{1}{R_{pt}}\right)A(T), \qquad (1)$$

where T is the saturation time, $A(T)=\int_0^T U_c(t)dt$ is the area under the curve in Figure 1b. For $T=550\,\mathrm{s}$ Eq. (1) gives $Q=9.26\cdot10^{-4}\,\mathrm{C}$, which allows to find the capacitance $C=Q/U_c(T)=9.08\cdot10^{-4}\,\mathrm{F}$. On the other hand, the capacitance of a parallel-plate capacitor is $C=\varepsilon_0\varepsilon(0)S/d$ which lets to find the dielectric constant $\varepsilon(0)=1.6\cdot10^6$ and dielectric

 doi:10.20944/preprints202404.1506.v1

susceptibility $\chi \approx 1.6 \cdot 10^6$. For comparison, the dielectric constant of borosilicate or phosphate glass is on the order of several units, and the maximum dielectric constant of ferroelectrics barely reaches 10^5. The current that is maintained for 550 s in the galvanically unconnected circuit cannot be anything other than an absorption current of mobile lithium ions. This is confirmed by two other plots in Figure 1b, recorded at temperatures of – 25° C and – 50° C. At low temperatures, in accordance with the Arrhenius law, the concentration of mobile lithium ions decreases as well as the lifetime of the absorption current. For the same reason, decreases the dielectric constant of LiPON. Thus, the alternating electric field creates an absorption current in the Pt|LiPON|Pt sandwich structure that cannot be ignored when interpreting LiPON impedance plots and simulating equivalent circuits.

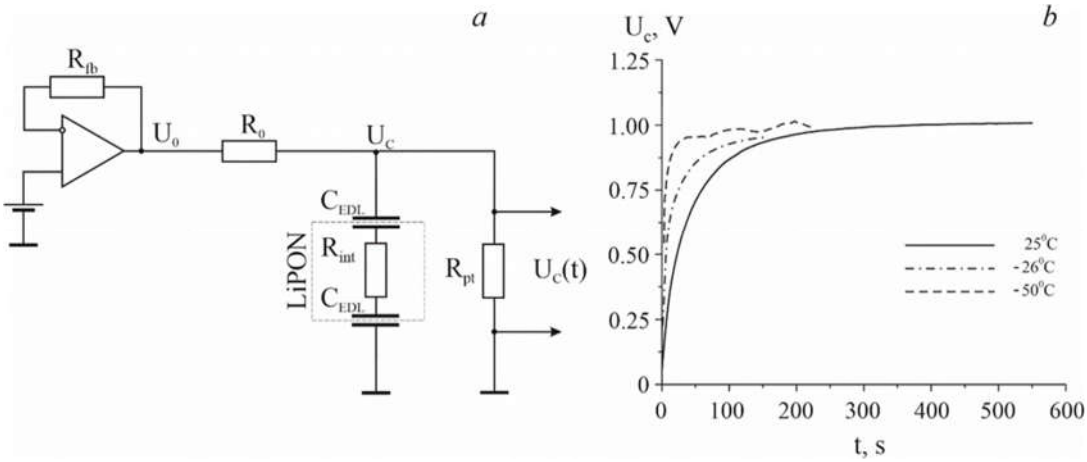

Figure 1. *a*) Scheme for measuring the absorption current and chemical capacity of the Pt|LiPON|Pt structure, where $U_0 = 1.18$ V, $R_0 = 100$ kΩ, $R_{pt} = 1$ MΩ. *b*) Time dependence of voltage across the Pt|LiPON|Pt structure [17].

2. Alternative Equivalent Circuit of LiPON

Figure 2*a* depicts the conventional equivalent circuit of the M|LiPON|M sandwich structure and an alternative circuit (Figure 2*b*) that considers the absorption current and the electric field screening by the electric double layer (EDL). Absorption element A determines both absorption and displacement currents, element W_1 simulates diffusion current. The capacitor C_{EDL}, which closes the AC current circuit, models the EDL capacitance, and the last two elements W_2 and R_{lk} form the leakage circuit. Resistor R_{lk} limits the rate of the Faraday process at the cathode while the Warburg element W_2 determines the diffusion rate of reduced lithium atoms to the anode. Resistor R simulates the "apparent" resistance which is related to intrinsic ohmic resistance as $R = \varepsilon(0) R_{int}$, where $\varepsilon(0)$ is LiPON dielectric constant. This equality follows from the independence of active resistance on frequency and is the only way to determine R_{int} in the case of electric field screening.

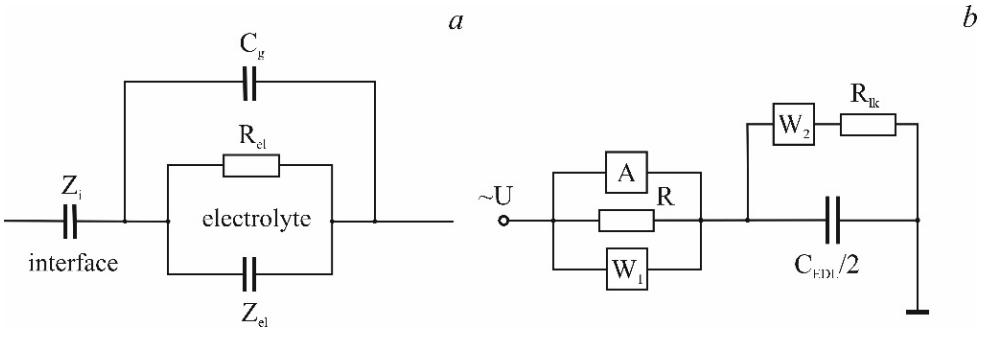

Figure 2. Equivalent circuits of the M|LiPON|M sandwich structure. *a*) conventional equivalent circuit of Pt|LiPON|Pt [5,8–15]. *b*) Alternative equivalent circuit where element A models the

 doi:10.20944/preprints202404.1506.v1

absorption and displacement current, elements R and W_1 determine drift and diffusion charge transfer, $C_{EDL}/2$ models two EDL in series, elements W_2 and R_{lk} form the leakage current circuit [17].

In Figure 2 W_1 and W_2 are a semi-infinite Warburg diffusion elements, the impedance of which are further designated as $Z_{W1,2} = Z'_{W1,2} + j\,Z''_{W1,2}$, where $Z'_{W1,2} = A_{W1,2}/\sqrt{\omega}$, $Z''_{W1,2} = -A_{W1,2}/\sqrt{\omega}$, $A_W = U_0/\sqrt{2DSqc_0}$ is the Warburg coefficient. Below, for brevity, the term "absorption" is used to denote the sum of absorption and displacement currents.

In accordance with the conventional algorithm, to strictly derive of an absorption element impedance, it is necessary to consider the boundary value problem on the electromagnetic wave propagation. Considering the heterogeneity of the medium in which $\vec{D}(x)$, such a problem seems difficult to solve. Therefore, further the absorption element is considered as a system with lumped parameters, for which the problem of medium inhomogeneity automatically vanishes. The absorption current is obtained as derivative of the electric induction

$$I_A = S\frac{dD}{dt} = j\omega S\varepsilon_0\varepsilon_{el}(\omega)E_0 e^{j\omega t}, \tag{2}$$

where $E_0 = U_0/d$, U_0 is the applied voltage, d is the LiPON thickness, S is electrode area, ω is the cyclic frequency, ε_{el} is dielectric constant of electrolyte, j is imaginary unit. The impedance is found as the ratio of voltage to absorption current

$$Z_A = \frac{d}{j\omega S\varepsilon_0\varepsilon_{el}(\omega)}. \tag{3}$$

To approximate the dielectric constant, the Cole and Cole model is used

$$\varepsilon_{el}(\omega) = \frac{\varepsilon_{el}(0) - \varepsilon_\infty}{1 + (j\omega\tau)^\beta} + \varepsilon_\infty \tag{4}$$

as appropriate for both resonant and relaxation oscillations [18], where τ is the relaxation time. The nonideality factor β is related to the corresponding parameter of Cole and Cole equation as $\beta = 1 - \alpha$. Substituting (3) into (2) allows to find the real and imaginary parts of the impedance Z_A

$$\begin{aligned} Z'_A &= \frac{A_A}{\omega}\frac{(1-\rho)(\omega\tau)^\beta \sin\left(\beta\frac{\pi}{2}\right)}{1 + 2\rho(\omega\tau)^\beta \cos\left(\beta\frac{\pi}{2}\right) + \rho^2(\omega\tau)^{2\beta}}, \\ Z''_A &= -\frac{A_A}{\omega}\frac{1 + \rho(\omega\tau)^{2\beta} + (1+\rho)(\omega\tau)^\beta \cos\left(\beta\frac{\pi}{2}\right)}{1 + 2\rho(\omega\tau)^\beta \cos\left(\beta\frac{\pi}{2}\right) + \rho^2(\omega\tau)^{2\beta}}, \end{aligned} \tag{5}$$

where $\rho = \varepsilon_\infty/\varepsilon_{el}(0)$, $A_A = d/S\varepsilon_0\varepsilon_{el}(0)$.

The total impedance $Z = Z' + jZ''$ of the circuit in Figure 3b is as follows

 doi:10.20944/preprints202404.1506.v1

$$Z' = R\frac{RZ'_{AW}+|Z_{AW}|^2}{(R+Z'_{AW})^2+Z''^2_{AW}}+\left(\frac{2}{\omega C_{EDL}}\right)^2\frac{R_{lk}+\frac{A_{W2}}{\sqrt{\omega}}}{\left(R_{lk}+\frac{A_{W2}}{\sqrt{\omega}}\right)^2+\left(\frac{A_{W2}}{\sqrt{\omega}}+\frac{2}{\omega C_{EDL}}\right)^2},$$
$$Z'' = \frac{R^2 Z''_{AW}}{(R+Z'_{AW})^2+Z''^2_{AW}}-\frac{2}{\omega C_{EDL}}\frac{\frac{A_{W2}}{\sqrt{\omega}}\left(\frac{A_{W2}}{\sqrt{\omega}}+\frac{2}{\omega C_{EDL}}\right)+\left(R_{lk}+\frac{A_{W2}}{\sqrt{\omega}}\right)^2}{\left(R_{lk}+\frac{A_{W2}}{\sqrt{\omega}}\right)^2+\left(\frac{A_{W2}}{\sqrt{\omega}}+\frac{2}{\omega C_{EDL}}\right)^2}, \quad (6)$$

where

$$Z'_{AW} = \frac{|Z_A|^2 Z'_{W1}+|Z_{W1}|^2 Z'_A}{(Z'_{dp}+Z'_{W1})^2+(Z''_{dp}+Z''_{W1})^2},$$
$$Z''_{AW} = j\frac{|Z_A|^2 Z''_{W1}+|Z_{W1}|^2 Z''_A}{(Z'_A+Z'_{W1})^2+(Z''_A+Z''_{W1})^2} \quad (7)$$

are the real and imaginary parts of the impedance of W_1 and A parallel connection, where

$$|Z_A|^2 = Z'^2_A+Z''^2_A,\ |Z_{W1,2}|^2 = 2\frac{A^2_{W1,2}}{\omega} \quad (8)$$

are module squares of absorption and Warburg impedances. Bode plots of Pt|LiPON|Pt impedance spectrum are shown in Figure 3*a*. The parameters of the approximating expressions (4) – (7) are given in the caption to the figure. The parameters R_{lk} and A_{w2} cannot be determined by fitting, because affect only the low-frequency part of the impedance spectrum, which is absent in an appropriate plot [5]. Figure 3*a* depicts in black the plots identical to experimental Bode diagrams by J. Bates et al. Colored curves are the plots of approximating expressions (5) – (8). According Figure 3*b* the inequality $R > \mathrm{Re}\,Z_W > \mathrm{Re}\,Z_A$ holds throughout the entire frequency range. Thus, the current in the circuit is determined by the absorption current, and not by drift or diffusion one.

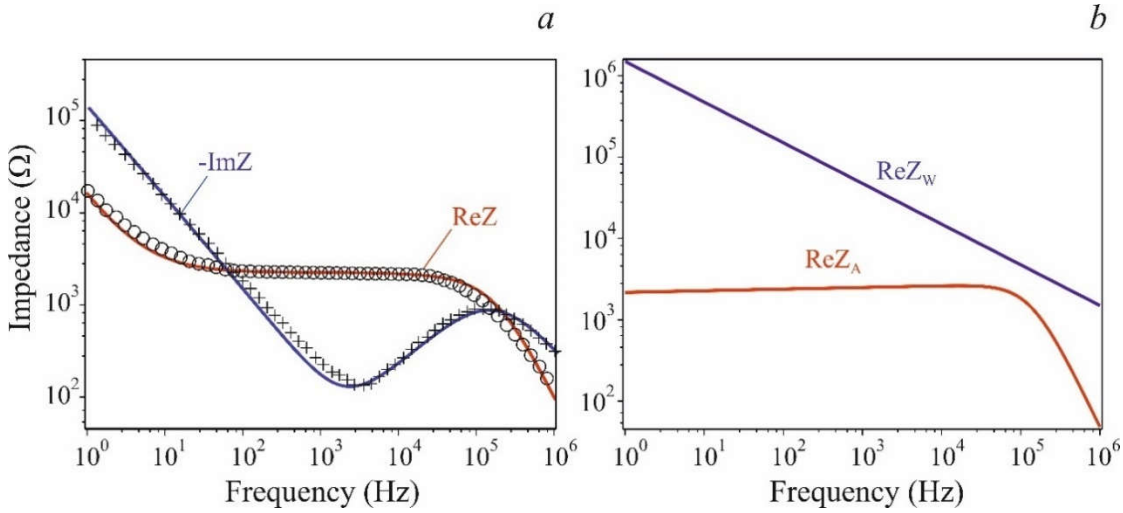

Figure 3. *a*) Real and imaginary parts of the LiPON impedance. The patterns in black depict the plots identical to Bode diagrams by J. Bates et al. [5]. The colored curves are the plots of the approximating equations (5) – (8) at parameters' values $\tau = 0.017$ s ; $\beta = 1.015$; $C_{EDL} = 9.7\cdot10^{-5}$ F ;

 doi:10.20944/preprints202404.1506.v1

$R=5\cdot10^{8}\ \Omega$; $\rho=3.5\cdot10^{-4}$; $A_{W1}=1.5\cdot10^{6}\ \Omega\cdot s^{-1/2}$; $A_A=1.31\cdot10^{5}\ \Omega\cdot s^{-1}$; R_{lk} and A_{W2} are not defined. b) $Re\,Z_A$ and $Re\,Z_{W1}$ Bode plots.

To verify the adequacy of the proposed model the fitting parameters can be compared with that of [5] and the results of direct measurements [17] (Table 1). Since in Figure 2*b* the ideal element $C_{EDL}/2$ models the capacitance of the entire Pt|LiPON|Pt sandwich structure, the relation $C_{EDL}/2=\varepsilon_0\varepsilon(0)S/d$ is valid, which allows to find the dielectric constant $\varepsilon(0)=C_{EDL}d/2S\varepsilon_0$. For $S=4\cdot10^{-6}$ m and $d=10^{-6}$ m this relation gives $\varepsilon(0)=1.37\cdot10^{6}$, which is very close to the result of direct measurements (Table 1). According to relation $R_{int}=R/\varepsilon(0)$ the intrinsic resistance is $R_{int}=3.65\cdot10^{2}\ \Omega$ and the corresponding conductivity is $\sigma_{int}=6.85\cdot10^{-6}\ S\cdot cm^{-1}$. This conductivity value can only be compared with theoretical results, or with calculations based on the lithium ions concentration and mobility data. For the diffusion coefficient $D=1.5\cdot10^{-11}\ cm^2\cdot s^{-1}$ [19] and the concentration $c=7.5\cdot10^{22}\ cm^{-3}$ obtained in [16] for the relation $Li/P=3.0$, the conductivity is $\sigma_{int}=7.0\cdot10^{-6}\ S\cdot cm^{-1}$, which is quite close to the conductivity obtained above.

Table 1. Fitting parameters of the equivalent circuit in Figure 2b in comparison with [5,17] data.

S, m²	d, m	C_{EDL}, μF	ε(0)	$\varepsilon_{el}(0)$	R, Ω	σ, S/cm	Reference
$4\cdot10^{-6}$	10^{-6}	97	$1.4\cdot10^{6}$	$2.0\cdot10^{3}$	365	$6.5\cdot10^{-6}$	Present work
$4\cdot10^{-6}$	10^{-6}	0.77	-	-	231.3	$2.3\cdot10^{-6}$	[5]
$6.4\cdot10^{-5}$	10^{-6}	908	$1.6\cdot10^{6}$	-	-	-	[17]

The real part of the impedance of the absorption element $Re\,Z_A$ (Figure 3*b*), which is responsible for dielectric losses, remains almost constant $Re\,Z_A=2.1\div2.6\ k\Omega$ over a wide frequency range from zero to tens of kilohertz. The corresponding conductivity belongs to the range of values $1.19\cdot10^{-6}\div9.6\cdot10^{-7}\ S\cdot cm^{-1}$. As one can see, dielectric losses are not much different from ohmic losses, since there is no fundamental difference between their mechanisms. Both are due to the dissipation of energy and momentum of free lithium ions. The only difference is that ohmic losses within this model are determined only at $\omega\to0$, and dielectric losses – over the entire frequency range. In addition, dielectric losses include energy and momentum dissipation by localized lithium ions, so in the low-frequency limit they do not turn into ohmic losses. Probably this is one of the reasons, why the resistance $Re\,Z_A$ is higher than R_{int} and the conductivity is lower than σ_{int}. The main reason is the ions density within the EDL and in the bulk.

3. Electric Double Layer

Equations (5) – (8) allow to generate any of Bode or Nyquist diagrams from those given in [5,8–15], but with different fitting parameters. First of all, this applies to the EDL capacitance, which increases by two orders of magnitude (Table 1) compared to [5]. In the cited works the nature of this capacity is uncertain. In the proposed equivalent circuit, this capacitance models a double electrical layer, to which the capacitance of the entire Pt|LiPON|Pt sandwich structure is assigned. There are several reasons why this capacity can be considered as EDL. Firstly, in all equivalent circuits this is ideal or almost ideal capacity. Secondly, this is a large ideal capacity, therefore, the gap between the plates of the appropriate parallel-plate capacitor must be on an atomic scale. Third, there are experimental evidences of lithium penetration across the metal-LiPON interface, which cannot but lead to EDL formation.

The very hypothesis of EDL is based on the fact that lithium comes out to the surface through any metal electrodes, including platinum. These facts include the products of lithium interaction with

 doi:10.20944/preprints202404.1506.v1

the atmosphere in the form of "prominences" [20] or "flower-like features" [11] formed on the surface. The starting point for constructing EDL model is the assumption that the transition of lithium ions into metal occurs as a result of diffusion and is accompanied by their reduction with the formation of metal ions layer, localized on the surface (Figure 4). These ions and charged cation vacancies bound by Coulomb forces form an EDL. Metal ions act as potential-determining ions, and cation vacancies act as counterions. The configuration of the layer of immobile cation vacancies is determined by the diffusion and drift of lithium ions, therefore the concept of "diffuse layer" is applicable to it. In essence, the EDL is a space-charge region, or depletion layer but in this context, considering it as a double electric layer is more appropriate.

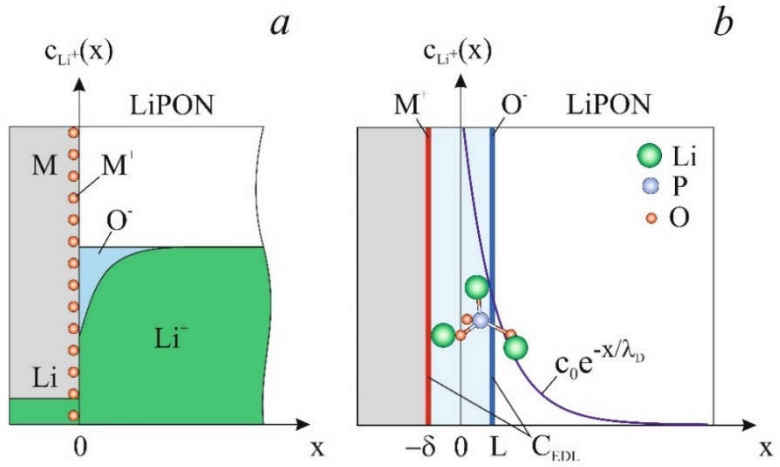

Figure 4. Model of the electrical double layer at the LiPON-metal interface. *a*) M^+ are potential-determining metal ions, O^- are cation vacancies (counterions). In blue is shown the diffuse layer formed by uncompensated cation vacancies (depletion layer). *b*) EDL simulation by plane capacitor, formed by metal ions layer and an imaginary plane $x = L$ passing through the center of mass of the counterions. The blue curve depicts the distribution of lithium concentration in the EDL region. The origin of coordinates is coincident with the plane formed by the centers of the Li ions.

Assumption that the metal ions are potential-determining enables the calculation of the cation vacancies concentration $c(x)$. Typically, the Poisson-Boltzmann equation is used for such calculations, which is applied to systems with a non-conserved number of particles. In this case, the number of cation vacancies is strictly equal to the number of potential-determining ions, and the consideration can be limited by Poisson equation. Since the concentration distribution in the EDL $c(x)$ is of greatest interest, the solution to the Poisson equation can be obtained last. The concentration can be calculated based on the obvious relation

$$E(x) = \frac{\rho_{pd}}{\varepsilon_0 \varepsilon} - \frac{q}{\varepsilon_0 \varepsilon} \int_0^x c(x)dx, \tag{9}$$

where ρ_{pd} is the surface density of potential-determining ions, q is the elementary charge, $c(x)$ is cation vacancies concentration. The field strength can be expressed from the equilibrium condition for diffusion and drift currents

$$\sigma E(x) = -qD\frac{dc(x)}{dx}, \tag{10}$$

where σ is the ionic conductivity of LiPON, D is the lithium diffusion coefficient. Note that here to the immobile cation vacancies is assigned the drift and diffusion mobility of lithium ions. Substituting (10) into (9) gives an integral-differential equation, which after differentiation takes the form of a diffusion equation

 doi:10.20944/preprints202404.1506.v1

$$\frac{d^2}{dx^2}c(x)-\frac{\sigma}{\varepsilon_0\varepsilon D}c(x)=0. \tag{11}$$

Solving equation (11) and satisfying condition $q\int_0^\infty c(x)dx=\rho_{pd}$ yields the concentration of cation vacancies, field strength, and potential in the EDL

$$c(x)=\frac{\rho_{pd}}{q}\frac{1}{\lambda_D}e^{-\frac{x}{\lambda_D}}, \tag{12}$$

$$E(x)=\frac{\rho_{pd}}{\varepsilon_0\varepsilon}e^{-\frac{x}{\lambda_D}}, \tag{13}$$

$$\left.\begin{aligned}\varphi(x)&=\frac{\rho_{pd}}{\varepsilon_0\varepsilon}\lambda_D e^{-\frac{x}{\lambda_D}},\ x\in[0,d-\delta]\\ \varphi(x)&=\frac{\rho_{pd}}{\varepsilon_0\varepsilon}(\lambda_D-x),\ x\in[-\delta,0]\end{aligned}\right\}, \tag{14}$$

where, $\lambda_D=\sqrt{\varepsilon_0\varepsilon_{el}(0)k_BT/q^2c_{Li}}$ is the Debye screening length, and δ is the shift of the coordinates origin from the metal surface (Figure 4). The parameter $\varepsilon_{el}(0)$ is the dielectric constant of the medium in which the concentration of free and localized lithium ions remains quite high. For LiPON with lithium concentration $c_{Li}\sim10^{28}\ m^{-3}$ the calculations give $\lambda_D=1.2\cdot10^{-11}\sqrt{\varepsilon_{el}(0)}\ m$. It is easy to verify that the solutions obtained satisfy the Poisson equation.

The EDL model makes it possible to calculate the capacitance of a double electrical layer as the capacitance of a parallel-plate capacitor, one of the plates of which is formed by potential-determining ions, and the other is an imaginary plane $x=L$ passing through the center of mass of the counterions (Figure 4*b*). The distance between these plates equals $L+\delta$, where $\delta=\ell+r_{Li}$, $\ell=2.03$? is the bond length of Li^+-O^- [21], $r_{Li}=1.45\cdot10^{-10}\ m$ is the radius of the lithium atom.

The parameter L can be obtained from the equation

$$\int_0^L c_{O^-}(x)dx=\int_L^\infty c_{O^-}(x)dx, \tag{15}$$

which gives $L=0.69\lambda_D$ or $L=8.3\cdot10^{-12}\sqrt{\varepsilon_{el}(0)}$. Considering (15), the expression for the EDL capacitance reduces to

$$C_{EDL}=\frac{\varepsilon_0\varepsilon_{el}S}{8.3\cdot10^{-12}\sqrt{\varepsilon_{el}}+\delta}. \tag{16}$$

For $S=4\cdot10^{-6}\ m^2$ capacitance (16) equals the fitting parameter $C_{EDL}=9.70\cdot10^{-5}\ F$ at $\varepsilon_{el}(0)=1.96\cdot10^3$. Finalizing the EDL topic, let's specify the value of the Debye shielding length $\lambda_D=5.31\cdot10^{-10}\ m$, the center of mass coordinate $L=3.66\cdot10^{-10}\ m$, and the distance between the plates of a parallel-plate capacitor, simulating the EDL $L+\delta=7.14\cdot10^{-10}\ m$.

 doi:10.20944/preprints202404.1506.v1

The dielectric constant of LiPON in the depletion layer and in the bulk can vary significantly. The relation $A_A = d / S\varepsilon_0\varepsilon_{el}(0)$ allows determining the dielectric constant of LiPON, which at $A_A = 1.31 \cdot 10^5\ \Omega \cdot s^{-1}$ proves to be $\varepsilon_{el} = 1.88 \cdot 10^4$. At $\rho = 3.5 \cdot 10^{-4}$ the appropriate value of the dielectric constant in the high frequency limit is $\varepsilon_\infty = 6.6$.

Another feature of the model proposed is that the best approximation of the curves in Figure 3 is achieved at $\alpha = -0.015$. This signifies that the appropriate dissipative element in Cole and Cole model, known as a constant phase element, is a weak kinetic inductance. Since the mode of mobile lithium ions oscillations is a relaxation one, the manifestation of kinetic inductance means a significant contribution of localized ions oscillations to the dielectric constant. It is also important that with $\omega \to 0$ the real part of absorption impedance $\mathrm{Re}\, Z_A \to 0$, while $\mathrm{Im}\, Z_A \to -\infty$, i.e., the absorption element passes into a conventional capacitor.

4. Summary

In conclusion, let us list the facts that testify in favor of the hypothesis about the absorption conductivity of LiPON and the existence of an electrical double layer. First of all, this is LiPON's high absorption capacitance. Also, this is a large value of static dielectric constant, which is an order of magnitude higher than the dielectric constant of ferroelectrics. Besides Bode diagrams generated using an alternative equivalent circuit containing an absorbing element reproduce in detail previously obtained experimental impedance spectra. The hypothesis eliminates the obvious discrepancy between the high dielectric constant of LiPON and equivalent circuits, which in no way consider the effect of electric field shielding in the low-frequency limit. The double electrical layer hypothesis allows to relate the high apperant ohmic resistance to the fairly high intrinsic conductivity of LiPON, which also follows from the impedance of the absorption element. The apparent resistance value obtained from the fitting almost completely coincides with the product of the dielectric constant and the internal resistance of LiPON. If the alternative LiPON impedance model is correct, then the conductivity results obtained in [5,8–15] should be attributed to dielectric losses.

Authors Contributions: A.S.R. – conceptualization, writing of original draft; A.V.N.— investigation. J.S.E. – investigation. All authors have read and agreed to the published version of the manuscript

Funding: This research was funded by the Ministry of Science and Higher Education of the Russian Federation grant number FENZ-2024-0005.

Data Availability Statement: Supporting reported results data can be found or obtained by de-mand at The Facilities Sharing Centre "Diagnostics of Micro- and Nanostructures" (FSC DMNS), P.G. Demidov Yaroslavl State University.

Conflicts of Interest: The authors declare that they have no conflicts of interest. The funders had no role in the design of the study; in the collection, analyses, or interpretation of data; in the writing of the manuscript, or in the decision to publish the results.

References

1. J.B. Bates, N.J. Dudney, G.R. Gruzalski, R.A. Zuhr, A. Choudhury, C.F. Luck, J.D. Robertson, Solid State Ionics **53-56**, 647 (1992).
2. J. Bates, N. Dudney, G. Gruzalski, R. Zuhr, A. Choudhury, C. Luck, J. Robertson, J. Power Sources **43**, 103 (1993).
3. J.B. Bates, G. R. Gruzalski, N.J. Dudney, C.F. Luck, Xiaohua Yu, Solid State Ionics, **70-71**, 619 (1994).
4. J.B. Bates, N.J. Dudney, D.C. Lubben, G.R. Gruzalski, B.S. Kwak, Xiaohua Yu, R.A. Zuhr, ibid. **54**, 58 (1995).
5. X.Yu, J.B. Bates, G.E. Jellison-Jr., F.X. Hart, J. Electrochem. Soc. **144**, 524–532 (1997). DOI: 10.1149/1.1837443.
6. Xiaohua Yu, J.B. Bates and G.E. Jellison, Proceedings of the Symposium on Thin Film Solid Ionic Devices and Materials, **95** (22), 23 (1995).
7. J.B. Bates, N.J. Dudney, C.F. Luck, B.C. Sales, R.A. Zuhr, J. Am. Ceram. SOC. **76,** 929 (1993).
8. Y. Hamon, A. Douard, F. Sabary, C. Marcel, P. Vinatier, B. Pecquenard, A., *Solid State Ionics*, **2006**, 177, 257.
9. Lin Li, Su Liu, Xin Xue, Hui Zhou, *Ionics* (2018) 24:351–362.
10. Nerea Mascaraque, José Luis G. Fierro, Alicia Durán, Francisco Muñoz, *Solid State Ionics*, 233 (2013) 73–79.

 doi:10.20944/preprints202404.1506.v1

11. C.S. Nimisha, G. Mohan Rao, N. Munichandraiah, Gomathi Natarajan, David C. Cameron, *Solid State Ionics*, 185 (2011) 47–51.
12. Lucie Le Van-Jodin, Frédérique Ducroquet, Frédéric Sabary, Isabelle Chevalier, *Solid State Ionics*, 253 (2013) 151–156.
13. F. Muñoz, A. Dur'an, L. Pascual, L. Montagne, B. Revel and A. C. M. Rodrigues, *Solid State Ionics*, **2008**, 179, 574.
14. B. Fleutot, B. Pecquenard, H. Martinez, A. Levasseur, *Solid State Ionics*, 206 (2012) 72–77.
15. Yurong Su, Jane Falgenhauer, Angelika Polity, Thomas Leichtweiß, Achim Kronenberger, Jaroslava Obel, Shengqiang Zhou, Derck Schlettwein, Jürgen Janek, Bruno K. Meyer, *Solid State Ionics*, 282 (2015) 63–69.
16. A. L´opez-Grande, G. C. Mather and F. Muñoz, *J. Mater. Chem. A*, 2023, 11, 12282.
17. A. S. Rudyi, M. E. Lebedev, A. A. Mironenko, L. A. Mazaletskii, V. V. Naumov, A. V. Novozhilova, I. S. Fedorov, and A. B. Churilov, *Russian Microelectronics*, 2020, 49, No. 5, 345.
18. Kenneth S. Cole; Robert H. Cole Dispersion and Absorption in Dielectricsıo 1. Alternating Current Characteristics. J. Chem. Phys. 9, 341–351 (1941).
19. A. Rudy, A. Mironenko, V. Naumov, A. Novozhilova, A. Skundin, I. Fedorov, Determination of Diffusion Coefficients of Lithium in Solid Electrolyte LiPON, Batteries 7 (2021) 1-8. doi:10.3390/batteries7020021
20. S.V. Vasilev, M.E. Lebedev, L.A. Mazaletskii, A.V. Metlitskaya, A.A. Mironenko, V.V. Naumov, A.V. Novozhilova, A.S. Rudyi, I.S. Fedorov, *Russian Microelectronics*, 2017, Vol. 46, No. 6, pp. 424–432.
21. Valentina Lacivita, Andrew Westover, Andrew K. Kercher, Nancy J. Dudney et al. Resolving the Amorphous Structure of Lithium Phosphorus Oxynitride (Lipon). Journal of the American Chemical Society 2018, 140 (35).